Supporting Information

Properties of APTES Modified CNC Films

Sadat Kamal Amit,[1] *Diego Gomez-Maldonado,*[2] *Tiana Bish,*[1] *Maria S. Peresin,*[2] *and Virginia A. Davis*[1*]

[1]Department of Chemical Engineering, 212 Ross Hall, Auburn University, Auburn, AL 36849, USA

[2]Sustainable Bio-Based Materials Lab, College of Forestry, Wildlife, and Environment, Auburn University, 602 Duncan Dr, Auburn, AL 36849, USA

* E-mail address: davisva@auburn.edu

Characterization

***CNCs dimensions*:** The length and height of individual CNCs were determined using an Anton Paar TOSCA 400 atomic force microscope (AFM). Samples were prepared by drop-casting a 15 ppm CNC dispersion onto a cleaved mica surface coated with poly-L-lysine. The substrate was rinsed with ultrapure water after 3 min and oven dried at 80 °C overnight. The samples were scanned in tapping mode, and Gwyddion was used to measure the dimensions by leveling the data and considering tip convolution. The length, height, and width of CNCs were 160 ± 36 nm, 3 ± 0.8 nm, and 57 ± 9 nm, respectively. A representative CNCs AFM image is shown in **Figure S1**.

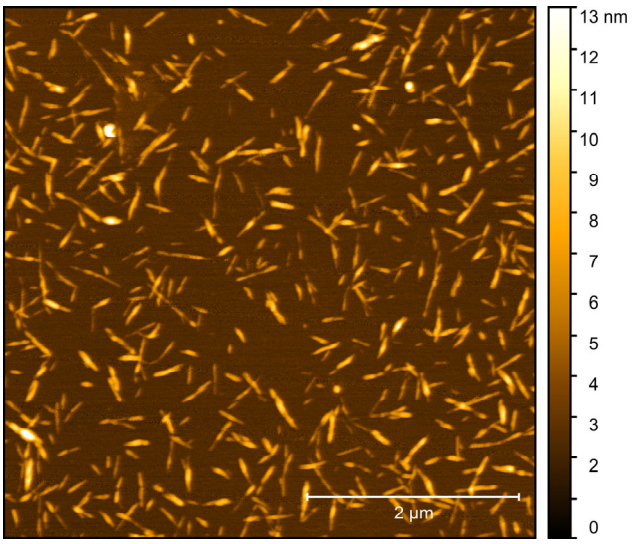

Figure S1. AFM scan of a dried 15 ppm CNC dispersion on mica surface coated with poly-L-lysine. Scale bar represents 2 µm.

Crystallinity Index: X-ray diffraction (XRD) was performed in an AXRD powder diffraction system (Proto Manufacturing) using Cu Kα (0.15418 nm) radiation generated at 40 kV and 30 mA in the range of 12 to 36 degrees for 2θ in 0.05-degree steps with a dwell time of 15 seconds.

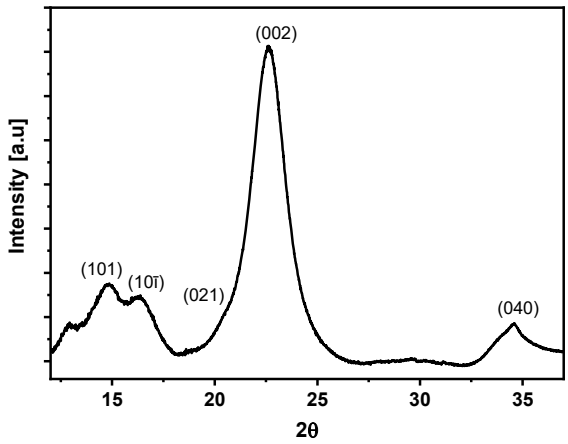

Figure S2. XRD spectra of CNCs with five distinct crystalline peaks.

The crystallinity index was determined from the XRD spectra by using a deconvolution method with curve fitting to find the areas under crystalline peaks and amorphous peaks along with Equation S1.

$$CI_R(\%) = \frac{A_c}{A_c + A_{am}} \times 100 \qquad \text{(Equation S1)}$$

where A_c is the total crystalline area, and A_{am} is the total amorphous area.

Sulfate half ester determination: The as received CNC gel was diluted to 1.5 wt% and dialyzed extensively with ultrapure water by placing the dispersion inside Spectra/Por 4 dialysis membrane and submersion into ultrapure water with gentle magnetic stirring. The water was changed every 12 hours until the dialyzed water pH became equal to the pH of pure water (pH = 6.4). DOWEX Marathon-C, a strong acid cation exchange resin, was used to prepare a column and thoroughly rinsed with ultrapure water. The dispersion was passed through the ion exchange column three times to protonate the CNCs. Next, a dispersion containing 150 mg of protonated CNCs (H-CNCs) was diluted with ultrapure water to result in a 200 mL dispersion. 2 mL of 0.1 M NaCl solution was added to increase the initial conductivity. Then, the dispersions were titrated with 10 mM NaOH using a Symphony B30PCI titrator system to determine the equivalent point, as shown in **Figure S3**. The sulfate half ester content was found to be 125 mmol $R-OSO_3^-$ per kilogram of CNCs (0.4 wt% S).

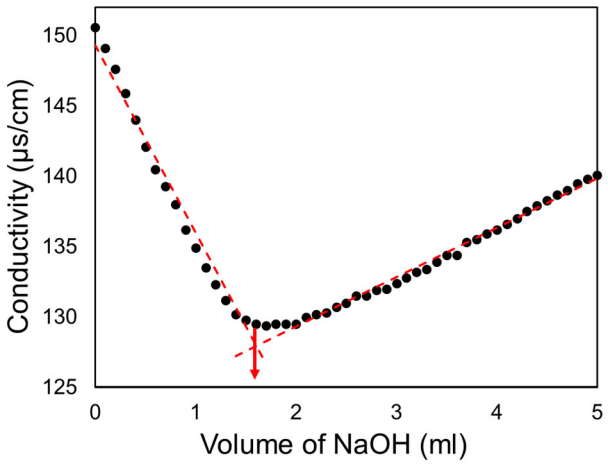

Figure S3. Conductometric titration plot of dispersion conductivity versus added volume of NaOH.

Charge density: Charge density was determined by colloidal titration using Chemtrac Laboratory Charge Analyzer. CNCs were diluted to form a 0.5 wt% aqueous dispersion, and 25 ml p-DADMAC (0.001N) was added to 15 ml of the CNC dispersion. The mixture was well mixed and centrifuged to remove any aggregates. 10 ml supernatant was collected and titrated against 0.001N PVSK in a charge analyzer. The charge density was calculated based on the volume required to make the dispersion charge neutral.

Thermal stability: A TA Instruments (New Castle, DE) TGA Q50 was used to determine the dispersion concentrations and thermal decomposition analysis of CNCs and CNC-APTES under Argon. The thermal degradation temperature was determined based on 5% mass loss after isothermal hold at 120°C. **Figure S4** provides a representative TGA plot of CNCs using an air atmosphere.

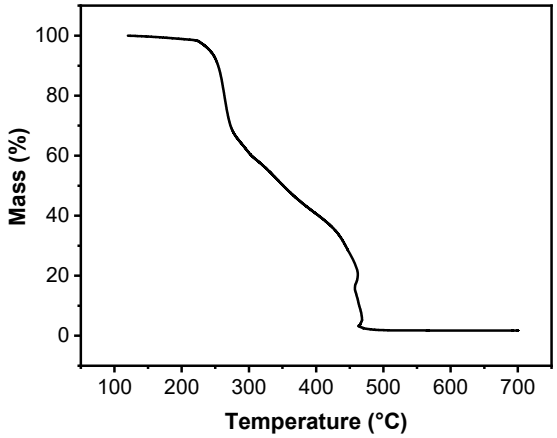

Figure S4. Thermal gravimetric analysis of CNCs in air.

Chemical Analysis: Oven-dried CNC and CNC-APTES samples ground using a mortar and pestle were used for attenuated total reflectance Fourier transform infrared spectroscopy (ATR-FTIR) and ultimate analysis. A PerkinElmer Spotlight 400 FTIR Imaging System (Massachusetts) with diamond/ZnSe crystal was used to collect 128 scans with 4 cm^{-1} resolution. A Vario MICRO cube CHNOS elemental analyzer was used to determine the nitrogen content in CNC-APTES. Freeze-dried CNC-APTES samples were analyzed by Intertek Pharmaceutical Services (Whitehouse, NJ) using inductively coupled mass spectroscopy (ICP-MS).

Dispersion Behavior: The zeta potential and hydrodynamic radius of CNCs and CNC-APTES were obtained for 0.01 wt% dispersions using a Litesizer from Anton-Paar (Gratz, Austria). A Nikon (Melville, NY) Eclipse Ni microscope equipped with a Nikon DS-RI2 camera and 20×/0.45 LU Plan Fluor objective was used to image the CNC and CNC-APTES dispersions. Aqueous dispersions of sulfated CNCs are known to follow lyotropic liquid crystalline phase behavior. The isotropic, biphasic, liquid crystal, and gel phase boundaries were estimated using cross-polarized optical microscopy. CNC-APTES did not show liquid crystalline phase behavior at any concentration. CNC-APTES dispersions appeared to show some aggregates (**Figure S6a**). AFM height images (**Figure S6b-c**) of CNC-APTES showed heights ranging from 3 - 22 nm compared to 3 nm for the sulfated CNC.

Table S1. Values and definition of the variables used in equation 1.

Symbol	Definition	Variable	Reference
L_1	Average Height of Individual CNC Nanorod	3 nm	AFM Characterization of Feedstock CNC
L_2	Average Width of Individual CNC Nanorod	57 nm	AFM Characterization of Feedstock CNC
L_3	Average Length of Individual CNC Nanorod	160 nm	AFM Characterization of Feedstock CNC
$d_{(110)}$	Horizontal Unit Cell of CNC	0.61 nm	Habibi et al., 2006 [3]
$d_{(1\bar{1}0)}$	Vertical Unit Cell of CNC	0.54 nm	Habibi et al., 2006 [3]
n_1	Number of primary -OH groups facing (110) in the unit cell	0.4843	Yoo et al., 2016 [4]
n_2	Number of secondary -OH groups facing (1$\bar{1}$0) in the unit cell	1.0066	Yoo et al., 2016[4]
ρ	Density of Crystalline Cellulose Iβ	1.605×10^{-21} g/nm^3	Yoo et al., 2016 [4]
c	Unit Cell Dimension	1.038 nm	Yoo et al., 2016 [4]
N_A	Avogadro's Number	6.02×10^{23} OH/mol	N/A

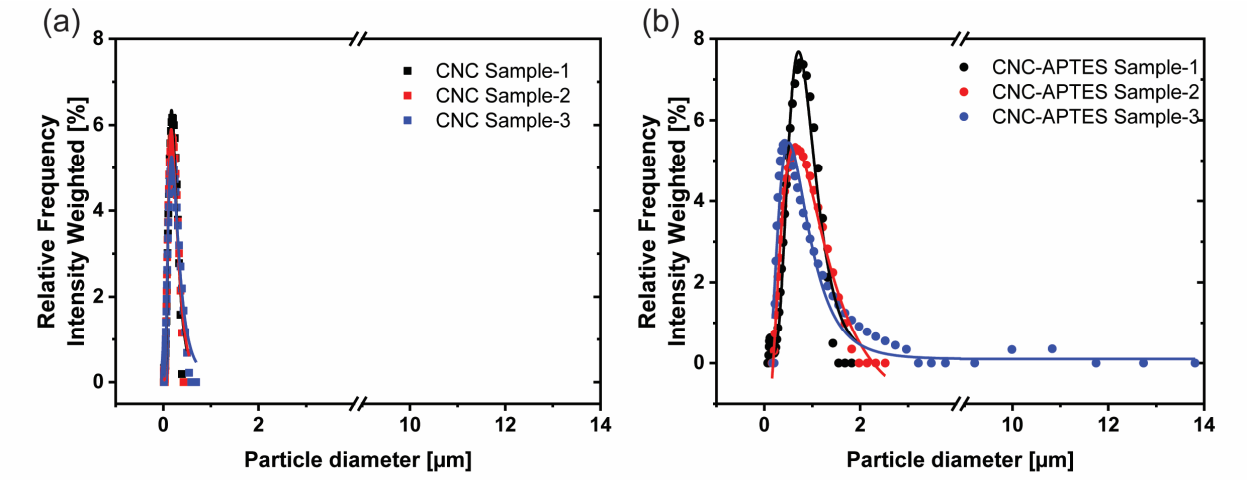

Figure S5. Size (hydrodynamic radius) distribution of (a) CNCs and (b) CNC-APTES obtained using dynamic light scattering (DLS). Solid lines represent the log-normal model fit data. R^2 value is greater than 0.95 for all the fits except CNC-APTES sample-3, which showed a second peak at around 10 µm. R^2 (CNC-APTES sample-3) is 0.94.

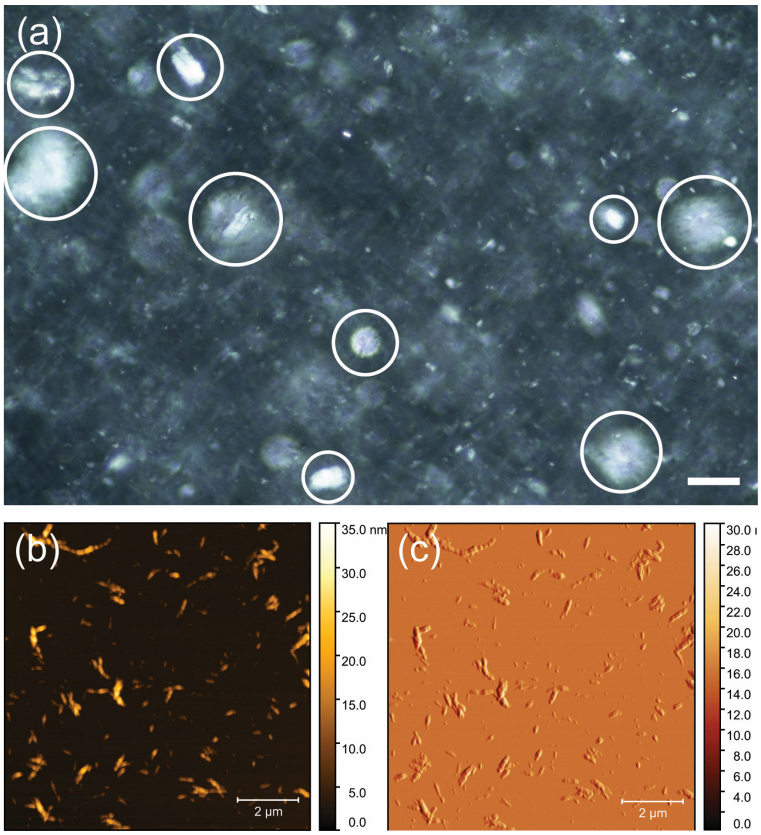

Figure S6. (a) Cross-polarized transmitted light microscopy of a 1.7 vol% (2.8 wt%) CNC-APTES dispersion. The aggregates are marked with white circles and appear larger than their actual size due to them not all being in the same focal plane. Scale bar represents 50 µm. AFM (b) height and (c) phase scan of CNC-APTES (15ppm) dried on mica substrate. Scale bar represents 2 µm.

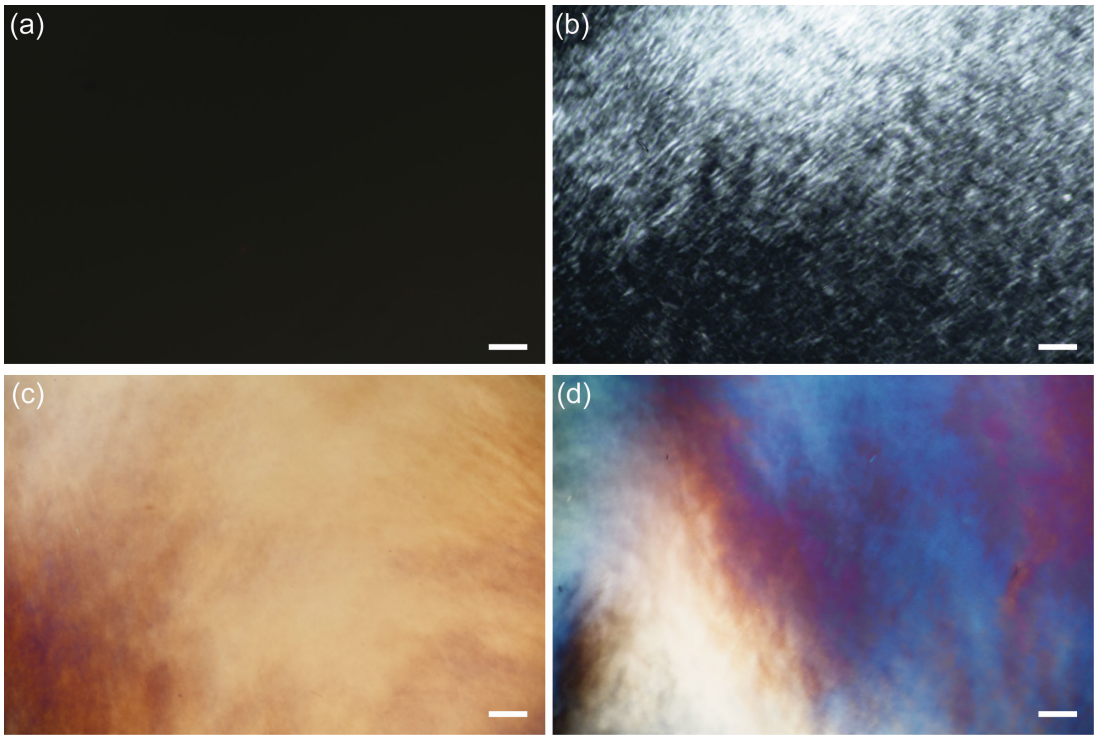

Figure S7. Representative transmitted cross-polarized optical microscopy images of aqueous CNC dispersions (a) isotropic (1.5 wt% / 0.9vol%, no areas of birefringence); (b) biphasic (3.5wt % / 2.2 vol%, both isotropic and ordered domains), (c) liquid crystal (5.0 wt % / 3.2 vol%, completely birefringent) and (d) gel (5.3wt % / 3.3vol%, paint texture) phases. Scale bar represents 50 µm.

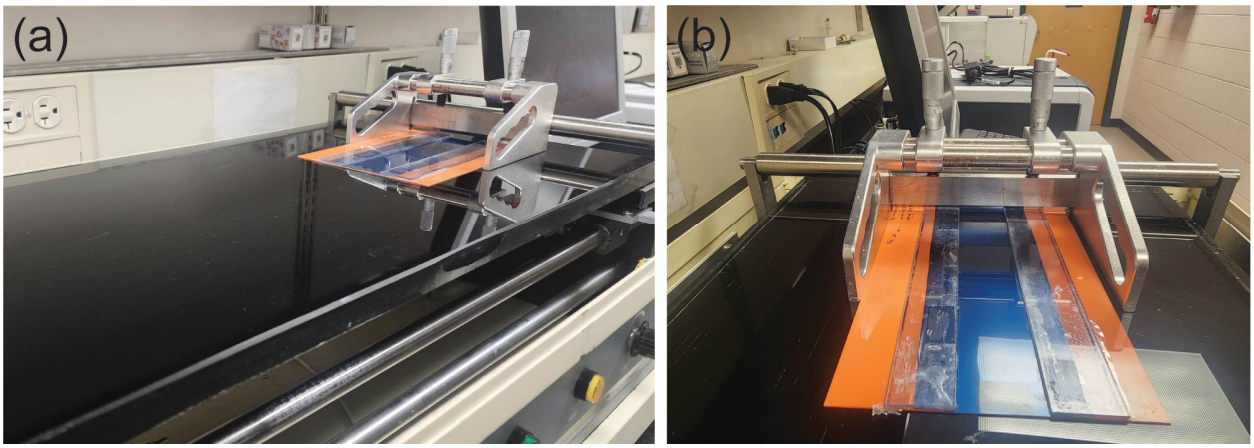

Figure S8. Image of film coater used for preparing shear cast CNC and CNC-APTES films; (a) MSK-AFA-II automatic thick film coater (MTI corporation), (b) Gardco film applicator on a polyester substrate.

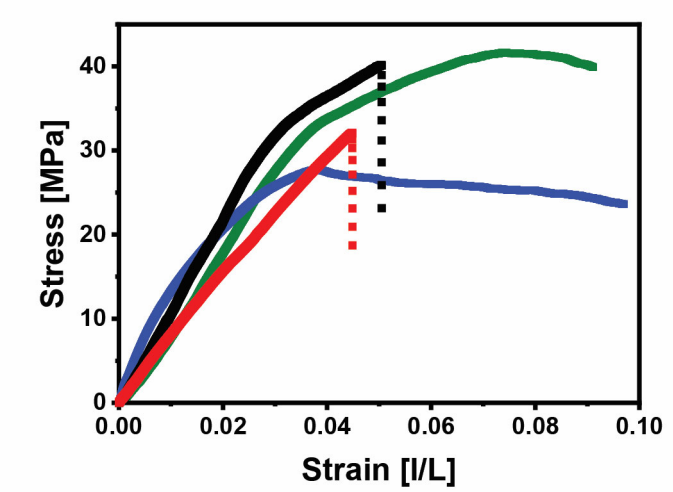

Figure S9. Representative stress-strain plot of shear cast CNC and CNC-APTES films before and water immersion (symbol key: ■ CNC before immersion, ■ CNC-APTES before immersion, ■ CNC-APTES 5 min immersion, ■ CNC-APTES 120 min immersion)

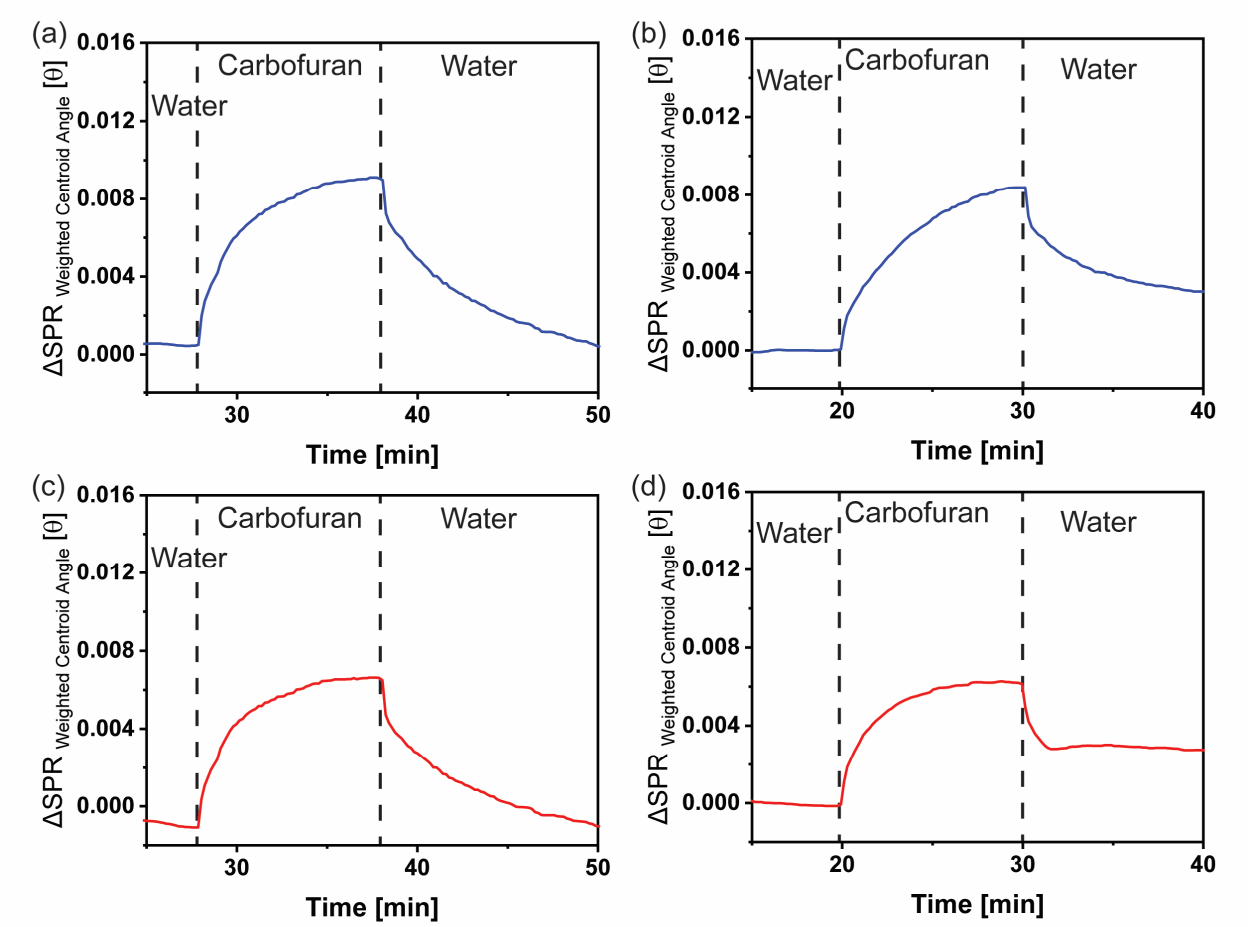

Figure S10. MP-SPR sensorgrams of CNC and CNC-APTES coated gold sensors; Interaction of carbofuran (100 ppm) with CNC film (a) channel 1, laser 785 nm (c) channel 2, laser 670 nm. Interaction of carbofuran (100 ppm) with CNC-APTES film (b) channel 1, laser 785 nm (d) channel 2, laser 670 nm.

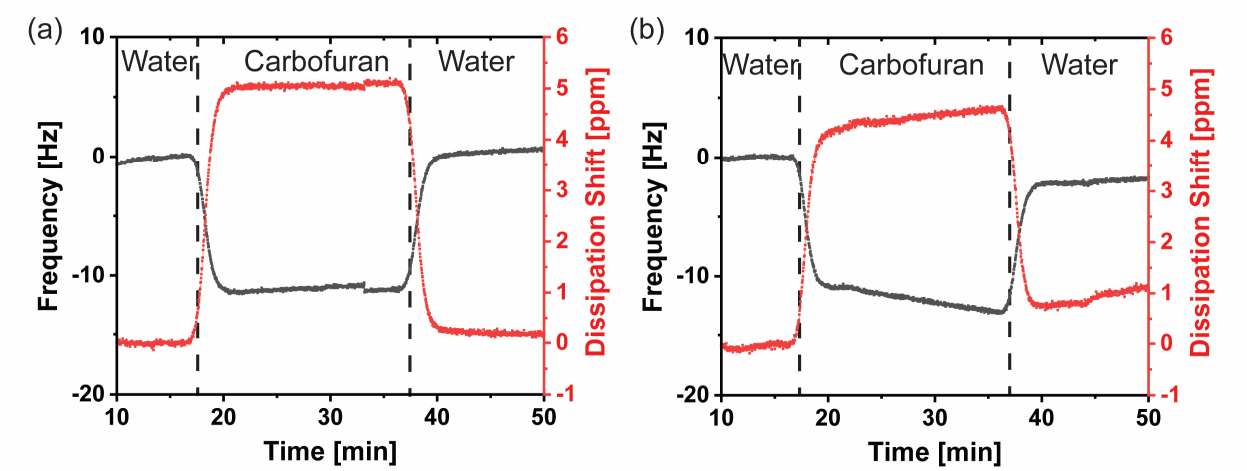

Figure S11. QCMD sensorgrams of CNC and CNC-APTES coated Au sensors; (a) QCMD: Interaction of carbofuran (100 ppm) with CNC film; (b) QCMD: Interaction of carbofuran (100 ppm) with CNC-APTES film. (Symbol key: ■ frequency, ■ dissipation).

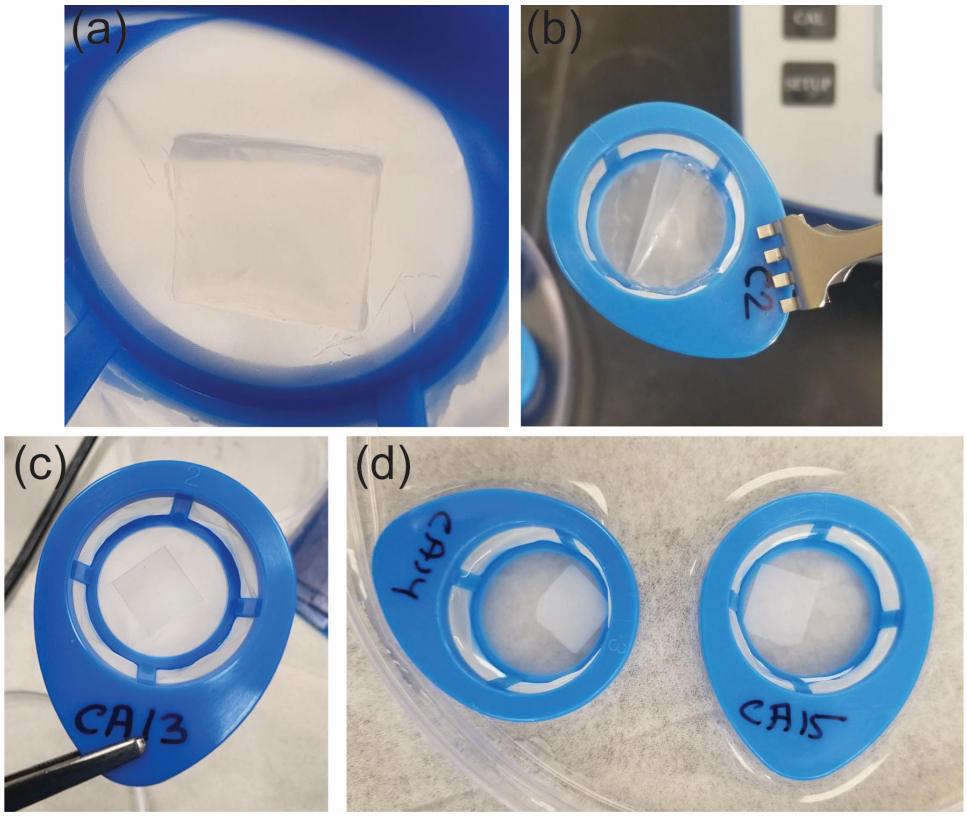

Figure S12. Hydrolytic stability testing of shear cast films. (a) Swelling of CNC films after 15 mins. (b) Change in shape of CNC films due to aqueous instability. (c) CNC-APTES film in a 40 µm nylon strainer. (d) CNC-APTES films immersed in water.

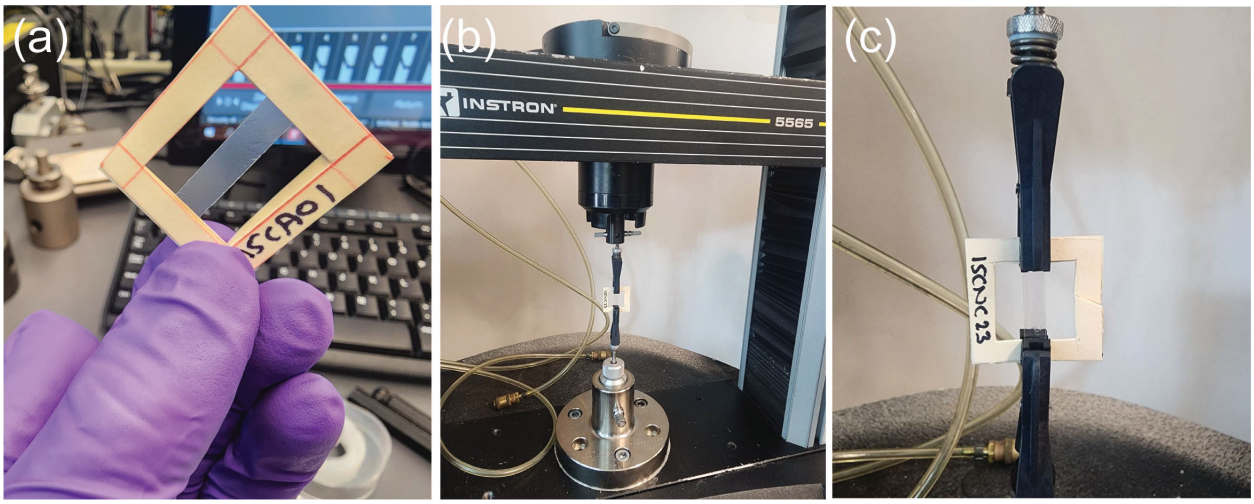

Figure S13. Tensile testing of shear cast films. (a) CNC-APTES film glued in a paper frame. (b-c) Frame with the filmed clamped for tensile testing in Instron 5565.

References

1. Foster, E. J.; Moon, R. J.; Agarwal, U. P.; Bortner, M. J.; Bras, J.; Camarero-Espinosa, S.; Chan, K. J.; Clift, M. J. D.; Cranston, E. D.; Eichhorn, S. J.; et al. Current characterization methods for cellulose nanomaterials. Chem. Soc. Rev. 2018, 47 (8), 2609-2679.
2. Eyley, S.; Thielemans, W. Surface modification of cellulose nanocrystals. *Nanoscale* 2014, *6* (14), 7764-7779.
3. Habibi, Y.; Chanzy, H.; Vignon, M. R. TEMPO-mediated surface oxidation of cellulose whiskers. *Cellulose* 2006, *13* (6), 679-687.
4. Yoo, Y.; Youngblood, J. P. Green one-pot synthesis of surface hydrophobized cellulose nanocrystals in aqueous medium. ACS Sustain. Chem. Eng. 2016, 4 (7), 3927-3938.